JOURNAL OF MATERIALS SCIENCE 19 (1984) 2719–2730

Effect of annealing on the superconducting properties of two amorphous alloys: $Nb_{70}Zr_{15}Si_{15}$ and $Zr_{85}Si_{15}$

A. INOUE, S. OKAMOTO*†, N. TOYOTA, T. FUKASE, K. MATSUZAKI*, T. MASUMOTO
The Research Institute for Iron, Steel and Other Metals, and Graduate School, Tohoku University, Sendai 980, Japan*

The changes in the superconducting and electronic properties of amorphous $Nb_{70}Zr_{15}Si_{15}$ and $Zr_{85}Si_{15}$ alloys with annealing were examined with an aim to evaluate the effect of structural relaxation on the superconductivity of metal–metalloid type amorphous alloys. T_c rises once from 3.99 to 4.42 K on annealing at temperatures below about 473 K for the Nb–Zr–Si alloy and from 2.71 to 2.75 K at temperatures below about 373 K for the Zr–Si alloy, and with further rising annealing temperature, t_d, lowers monotonically to a final relaxed value ($\simeq$ 3.15 K for $Nb_{70}Zr_{15}Si_{15}$ and $\simeq$ 2.49 K for $Zr_{85}Si_{15}$), which is independent of the previous thermal cycling. These results indicate that the thermal relaxation of an amorphous phase occurs through at least two stages. The lowering of T_c occurs exponentially with t_d, and an activation energy for the relaxation process and the frequency of jump over the barrier were estimated to be about 2.03 eV and 2.4×10^{14} sec^{-1} for $Nb_{70}Zr_{15}Si_{15}$ and about 1.28 eV and 1.2×10^{11} sec^{-1} for $Zr_{85}Si_{15}$, respectively. The high frequencies indicate that the relaxations occur more or less independently of each other in a non-co-operative manner. The dressed density of electronic states at the Fermi level, $N(E_f)(1 + \lambda)$, which was calculated from the measured values of ρ_n and $(dH_{c2}/dT)_{T_c}$, exhibited a similar annealing temperature dependence to that of T_c. From this the change in T_c on thermal relaxation was interpreted as due to the changes in λ and/or $N(E_f)$. From the depressions of $J_c(H)$ and fluxoid pinning force on annealing in a temperature range of 473 to 873 K, it was concluded that the structural relaxation from a less homogeneous quenched-in state to a homogeneous stable state occurred on the scale of coherence length ($\simeq$ 7.5 nm) during the annealing.

1. Introduction

It has become clear in recent years that mechanical, magnetic and electrical properties as well as the structure of amorphous alloys change significantly upon annealing at temperatures much below crystallization temperature because of the thermodynamically metastable state of the amorphous phase [1]. Since the superconducting properties are also very structure-sensitive, it is expected that they might be strongly affected by the change in microscopic structure upon low-temperature annealing. Further, the researches on the change in the superconducting properties by thermal relaxation offer useful information on the structural change in the annealed amorphous phase. Up to date, a few investigations have been reported on the influence of thermal relaxation on the superconducting properties in some amorphous alloys such as Zr–Rh [2], Zr–Ni [3] and Mo–Ru–B [4] systems. According to their results, the

†Present address: Fujitsû Ltd, Kawasaki 211, Japan.

superconducting transition temperature (T_c) of the zirconium-based and molybdenum-based amorphous alloys lowers monotonically with proceeding thermal relaxation. More recently, we have carried out a systematic research on the influence of low-temperature annealing on the superconducting properties of metal–metalloid type amorphous alloys of niobium-based and zirconium-based systems and have found that the change in T_c upon annealing is distinguished by two stages; T_c rises at first and then lowers with proceeding annealing. This result is not always consistent with the previous data [2–4] of Zr–Rh, Zr–Ni and Mo–Ru–B amorphous alloys which show only a monotonic lowering of T_c. In this paper, we present the results of the effect of thermal relaxation on the superconducting properties of T_c, upper critical magnetic field, $H_{c2}(T)$, critical current density, $J_c(H)$, and flux flow resistivity, $\rho_f(H)$, for amorphous $Nb_{70}Zr_{15}Si_{15}$ and $Zr_{85}Si_{15}$ alloys. The two alloys were chosen because they exhibited typical characteristics of an amorphous superconductor [5, 6] and rather high crystallization temperatures [7] which enable them to be annealed in a wide temperature range.

2. Experimental methods

The amorphous superconductors selected for this study are $Nb_{70}Zr_{15}Si_{15}$ (at %) and $Zr_{85}Si_{15}$ alloys, and the superconducting properties of T_c, the transition width and the H_{c2} gradient near T_c $[-(dH_{c2}/dT)_{T_c}]$ are 3.99 K, 0.15 K and 1.67×10^6 A m^{-1} K^{-1} (2.10 T K^{-1}) for $Nb_{70}Zr_{15}Si_{15}$, and 2.71 K, 0.05 K and 2.30×10^6 A m^{-1} K^{-1} (2.89 T K^{-1}) for $Zr_{85}Si_{15}$, respectively. Additionally, the crystallization temperature (T_x) was 1030 K for the niobium-based alloy and 759 K for the zirconium-based alloy. T_x is defined as the onset temperature of the exothermic peak on the differential thermal analysis (DTA) curve measured at a heating rate of 40 K min^{-1}. The master ingots of the two alloys were made under a purified and gettered argon atmosphere in an arc furnace on a water-cooled copper mould from niobium (99.5 wt %), zirconium (99.6 wt %) and silicon (99.999 wt %). The ingots were repeatedly turned over and remelted to ensure homogeneity. The compositions of alloys reported are the nominal ones since the losses during melting were negligible.

The technique and apparatus for fabricating ribbon samples with a typical cross-section of about 20 μm × 1 mm and the method of characterizing the amorphous nature of the samples by DTA, X-ray and electron metallographic techniques have been described elsewhere [8, 9]. The change in the superconducting properties upon annealing was examined on specimens annealed for various periods of 1 to 100 h at different temperatures in the range of 373 to 1073 K in evacuated quartz capsules. All measurements of superconducting properties T_c, $J_c(H)$, $H_{c2}(T)$ and $\rho_f(H)$ were done resistively using a conventional four-probe technique. The critical current was defined as the threshold current at which no-zero voltage ($\simeq 1$ μV) was first detected. The temperature was measured within an accuracy of ± 0.01 K using a calibrated germanium thermometer. The magnetic field up to 7.2×10^6 A m^{-1} (9.0 T) was applied perpendicularly to the specimen surface and feed current. The cross-sectional area was measured using optical microscopy in order to minimize error in the estimation of the electrical resitivity.

3. Results

3.1. Superconducting transition temperature (T_c)

Fig. 1 shows the normalized electrical resistance near T_c for a series of amorphous $Nb_{70}Zr_{15}Si_{15}$ samples annealed for 1 h at different temperatures ranging from 373 to 1073 K. We defined T_c as the temperature corresponding to $R/R_n = 0.5$, where R_n is the resistance in the normal state. The transition occurs rather sharply with a temperature width of less than about 0.2 K and there is no systematic change in the transition behaviour from normal to superconductive state with annealing temperature. T_c and normal electrical resistivity (ρ_n) just above T_c of the $Nb_{70}Zr_{15}Si_{15}$ alloy obtained from the data in Fig. 1 are plotted as a function of annealing temperature in Fig. 2, where the transition boundaries from amorphous single state to the state including crystalline phase determined by X-ray diffraction are also shown for reference. Upon annealing, T_c rises at first by about 0.4 K in the range of 373 to 473 K and then lowers in the range of 573 to 873 K. A slight rise of T_c at 973 K originates from the precipitation of superconductive βNb(Zr) particles with a bcc structure [10] into the amorphous matrix. It is noteworthy in Fig. 2 that the T_c value of the amorphous alloy exhibits a difference of as large as about 1.3 K, even in the amorphous single state. Fig. 2 also shows the change in the normal electrical resistivity (ρ_n) at temperatures just above T_c

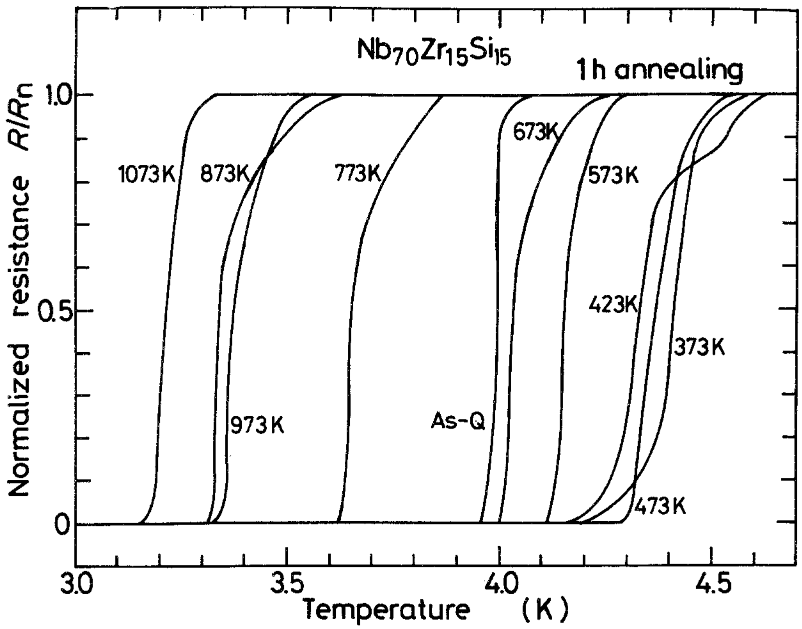

Figure 1 Normalized electrical resistance, R/R_n, near T_c for an amorphous $Nb_{70}Zr_{15}Si_{15}$ alloy annealed for 1 h at various temperatures.

as a function of annealing temperature. The ρ_n decreases monotonically from 1.90 to 1.75 $\mu\Omega$m in a temperature range below about 800 K, then exhibits a slightly higher value $\simeq 1.8$ $\mu\Omega$m in the vicinity of the temperature just before the crystallization starts and decreases rapidly down to 1.0 $\mu\Omega$m after crystallization.

A similar change in T_c with annealing temperature was observed for an amorphous $Zr_{85}Si_{15}$ alloy. The results are shown in Figs. 3 and 4. T_c rises by about 0.05 K on annealing at a temperature as low as 373 K, while the subsequent annealing causes a lowering from 2.75 to 2.49 K, even in the amorphous state. Further, one can notice in Fig. 4 that T_c is lowered significantly down to 1.4 K by the transition from amorphous to crystalline phase. The maximum difference in T_c in the amorphous single state of the $Zr_{85}Si_{15}$ alloy is about 0.26 K, being about a fifth of that (1.3 K) of $Nb_{70}Zr_{15}Si_{15}$ alloy.

Fig. 5 shows the changes in T_c and transition width of a series of $Nb_{70}Zr_{15}Si_{15}$ samples upon

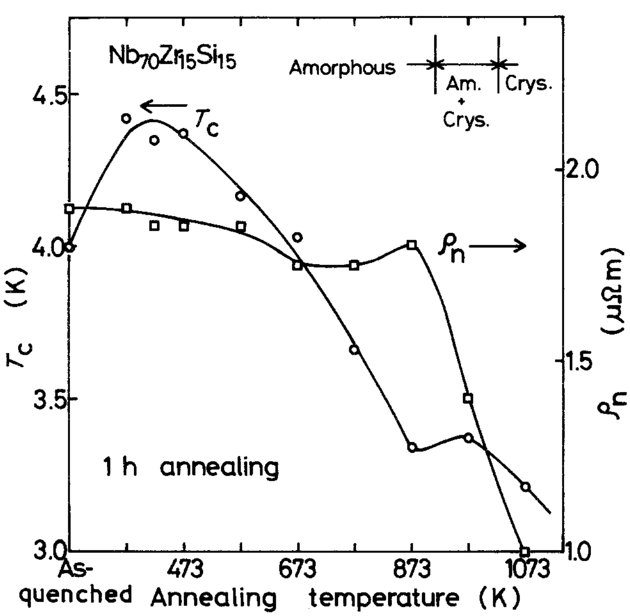

Figure 2 Changes in the superconducting transition temperature (T_c) and normal electrical resistivity just above T_c (ρ_n) of an amorphous $Nb_{70}Zr_{15}Si_{15}$ alloy with annealing temperature.

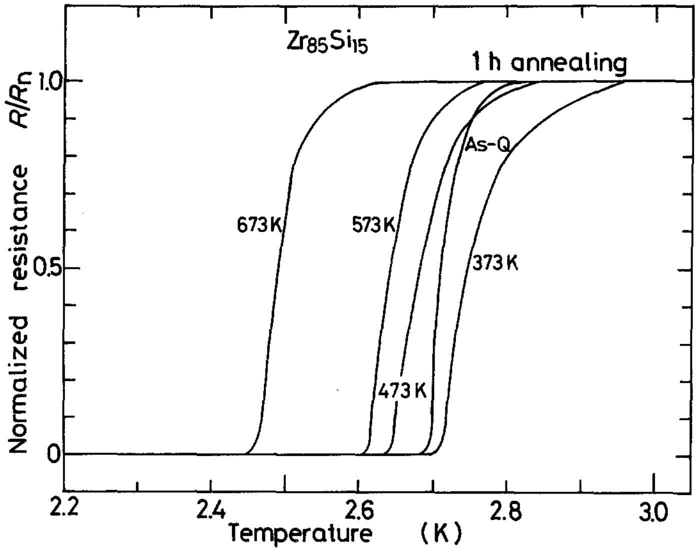

Figure 3 Normalized electrical resistance, R/R_n, near T_c for an amorphous $Zr_{85}Si_{15}$ alloy annealed for 1 h at various temperatures.

isothermal annealing for 1 to 100 h at various temperatures. The open markings represent an amorphous single state, the closed markings a crystalline state and the semi-closed markings a duplex state of amorphous and crystalline phases. T_c rises from 3.99 to 4.62 K with annealing time in the range of 373 to 573 K, whereas the annealing at temperatures above 673 K results in a lowering to a final relaxed value of $\simeq 3.15$ K. The T_c rises most remarkably at 373 K and the rise is as large as 0.63 K after annealing for 100 h. Further, it is very important to note that the T_c values of the fully relaxed amorphous alloy annealed at a temperature just below the crystallization temperature exhibit a nearly constant value ($\simeq 3.15$ K), which is independent of the previous thermal conditions. In Fig. 5, the rise of T_c for the alloy annealed for 100 h at 873 K is due to the precipitation of crystalline βNb(Zr) particles into the amorphous matrix. The appearance of crystalline phase after annealing for 100 h at 873 K is also supported by the disappearance of the flux flow resistivity, which is a typical characteristic for the amorphous phase, because the large fluxoid pinning force of the βNb(Zr) superconductive phase obstructs the generation of flux flow resistivity. The vertical bars in Fig. 5 represent the transition width and there is no appreciable systematic change in transition width upon isothermal annealing at various temperatures.

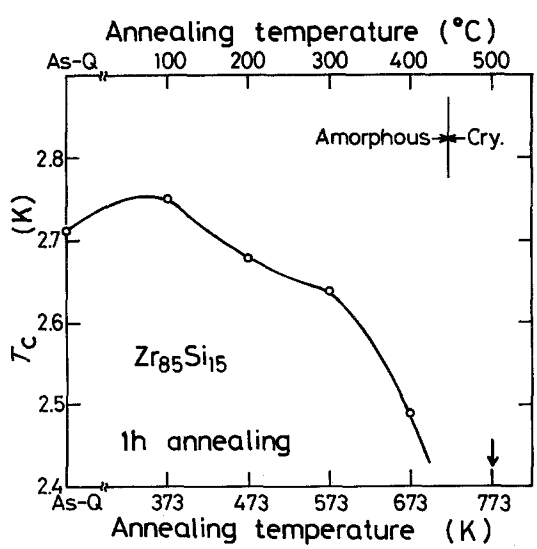

Figure 4 Change in the T_c of an amorphous $Zr_{85}Si_{15}$ alloy with annealing temperature.

A similar change in T_c upon isothermal annealing was observed for a series of $Zr_{85}Si_{15}$ samples. As shown in Fig. 6, T_c of the alloy annealed at 373 K rises at first and then lowers, while the annealing at temperatures above 473 K results in a monotonic lowering of T_c. The largest rise of T_c is about 0.24 K for the alloy annealed for 10 h at 373 K. Further, one can easily notice that the T_c values in the annealed state just before crystallization exhibit a nearly constant value of $\simeq 2.5$ K.

Considering the change in T_c upon the isothermal and isochronal annealings (Figs. 5 and 6), it may be concluded that the T_c values of the amorphous alloys exhibit a nearly constant value in a fully relaxed structural state and are independent of the quenched-in defect structure. The ratio of the difference between the highest T_c value and the T_c value of the alloy annealed for a period of

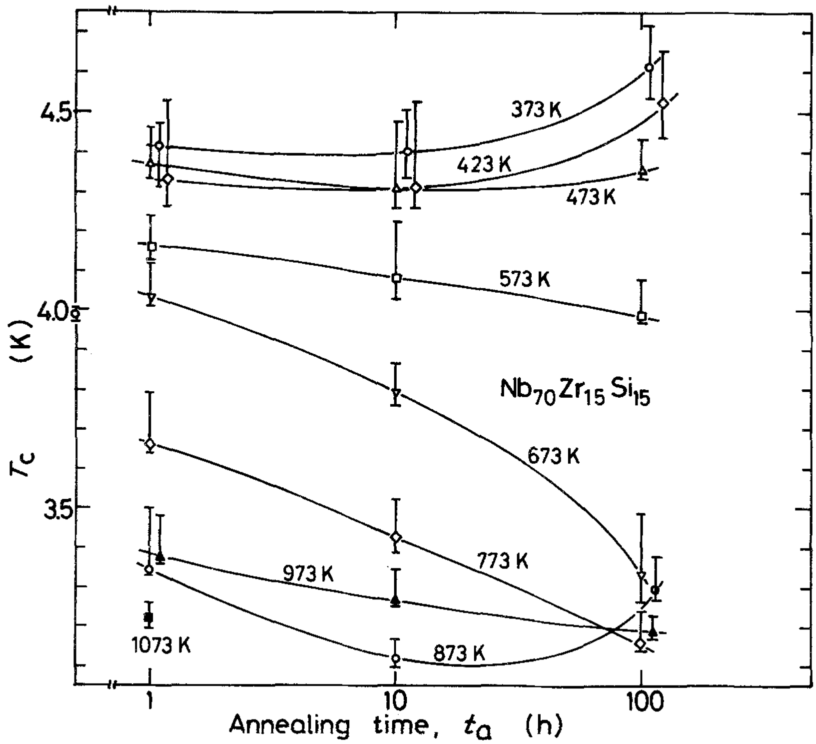

Figure 5 Changes in the T_c and transition width of an amorphous $Nb_{70}Zr_{15}Si_{15}$ alloy as a function of annealing time at various temperatures. Vertical bars represent the transition width.

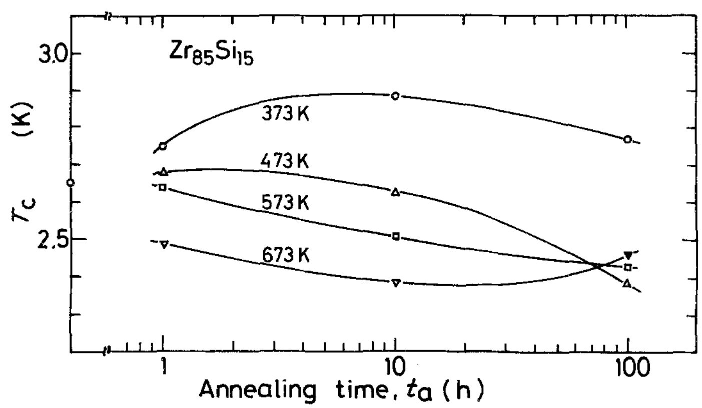

Figure 6 Change in the T_c of an amorphous $Zr_{85}Si_{15}$ alloy as a function of annealing time at various temperatures.

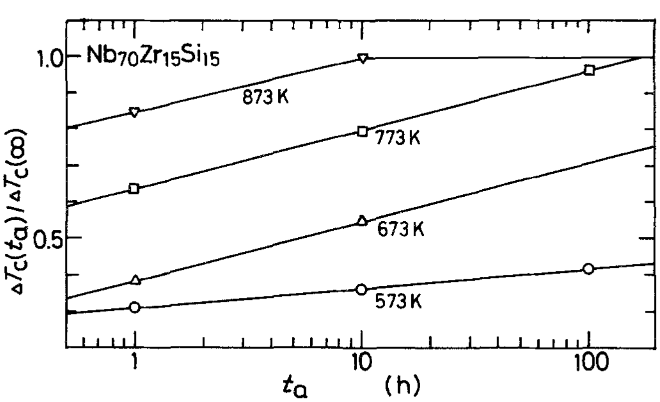

Figure 7 Change in the degradation ratio of T_c of an amorphous $Nb_{70}Zr_{15}Si_{15}$ alloy as a function of logarithm of annealing time at various temperatures.

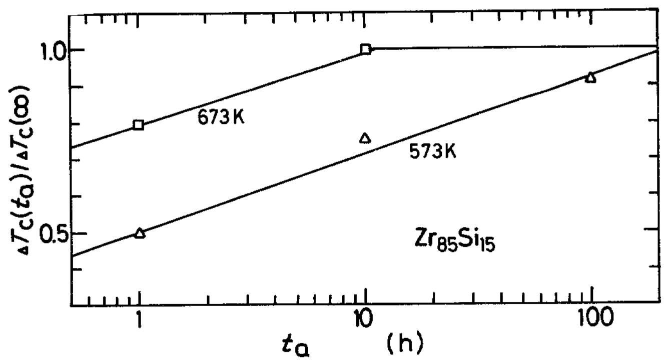

Figure 8 Change in the degradation ratio of T_c of an amorphous $Zr_{85}Si_{15}$ alloy as a function of logarithm of annealing time at various temperatures.

t_a [$\Delta T_c(t_a)$] to the largest difference between the highest- and the lowest-T_c values [$\Delta T_c(\infty)$] is plotted as a function of the logarithm of annealing time (t_a) at different temperatures in Fig. 7 for $Nb_{70}Zr_{15}Si_{15}$ and in Fig. 8 for $Zr_{85}Si_{15}$. As seen in the figures, there exists a rather good linear relation between $\Delta T_c(t_a)/\Delta T_c(\infty)$ and log t_a in the temperature range of 573 to 873 K for the Nb–Zr–Si alloy and in the range of 573 to 673 K for the Zr–Si alloy.

3.2. Upper critical field (H_{c2})

Fig. 9 shows the temperature dependence of H_{c2} near T_c for a series of $Nb_{70}Zr_{15}Si_{15}$ samples

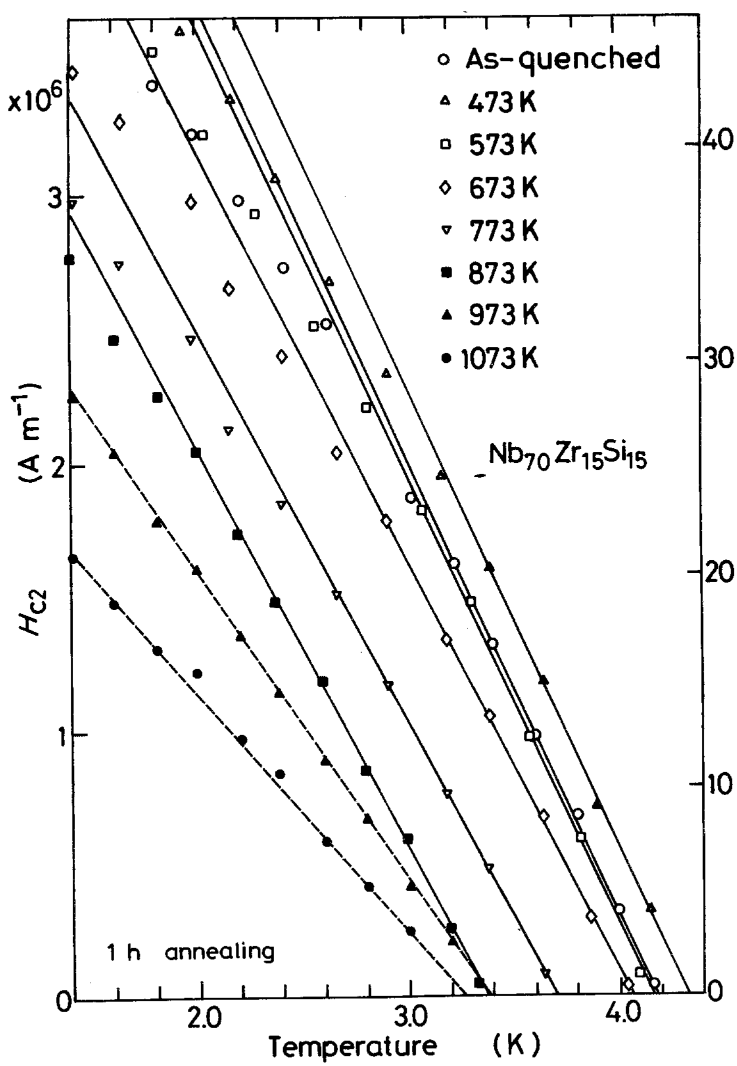

Figure 9 Temperature dependence of upper critical field, H_{c2}, of an amorphous $Nb_{70}Zr_{15}Si_{15}$ alloy annealed for 1 h at various temperatures.

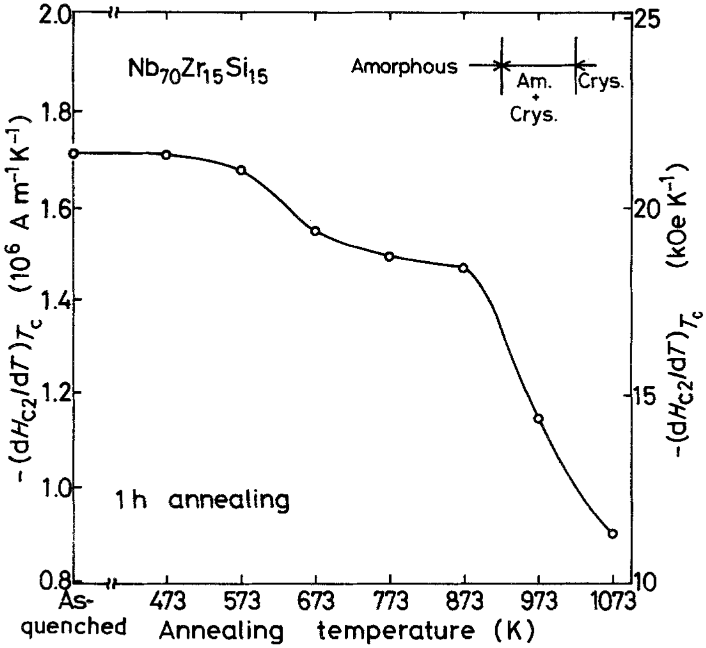

Figure 10 Change in the temperature gradient of H_{c2} near T_c, $-(dH_{c2}/dT)_{T_c}$, of an amorphous $Nb_{70}Zr_{15}Si_{15}$ alloy as a function of annealing temperature.

annealed for 1 h at different temperatures ranging from 473 to 1073 K. The solid and dashed lines represent a linear relation of $H_{c2}(T)$ near T_c for the amorphous and crystalline phases, respectively. In both the amorphous and crystalline states, the H_{c2} near T_c increases linearly with lowering temperature. The $-(dH_{c2}/dT)_{T_c}$ values of the $Nb_{70}Zr_{15}Si_{15}$ amorphous alloy are shown as a function of annealing temperature in Fig. 10. The gradient hardly changes in the range below 573 K, but with further rising temperature slightly decreases in the amorphous state and then decreases significantly after crystallization.

3.3. Critical current density $J_c(H)$ and flux flow resistivity $\rho_f(H)$

Fig. 11 shows the magnetic field dependence of J_c in the vicinity of 1.40 K for the $Nb_{70}Zr_{15}Si_{15}$ amorphous alloy in the as-quenched state and in the annealed states for 1 h at 473 K where the rise of T_c was observed, and at 773 and 873 K where T_c lowers rather largely. Although the $J_c(H)$ is slightly higher for the annealed state at 473 K than for the as-quenched state over the whole magnetic field range, the further rise of annealing temperature causes a significant depression of $J_c(H)$ values. This indicates that the fluxoid pinning force in the amorphous phase becomes weak with proceeding thermal relaxation. Fig. 12 shows the plot of ρ_f/ρ_n of the $Nb_{70}Zr_{15}Si_{15}$ alloy in as-quenched and annealed states as a function of magnetic field (H). The arrows in the figure represent the H_{c2} value at 1.40 K. There is no significant difference in $\rho_f(H)$ behaviour between the as-quenched sample and the annealed sample at 473 K, but the sample annealed at 773 K exhibits $\rho_f(H)$ values considerably higher than that of the former two samples. Such a difference indicates clearly that the generation of the flux flow resistivity for the amorphous superconductor becomes much easier on thermal relaxation, being consistent with the result (Fig. 11) that the thermal relaxation causes a significant depression of $J_c(H)$. By using the linear field dependence of ρ_f/ρ_n shown in Fig. 12, we can estimate the $H^*_{c2}(0)$, which is the hypothetical upper critical field determined only by the orbital effect, from Kim's empirical law [11], $\rho_f/\rho_n = H/H^*_{c2}(0)$. As a result, the $H^*_{c2}(0)$ is about 9.55×10^6 A m^{-1} (12.0 T) for the as-quenched and annealed (473 K) samples and 6.77×10^6 A m^{-1} (8.5 T) for the sample annealed at 773 K. Thus, the $H^*_{c2}(0)$ value hardly changes upon annealing below 473 K, but decreases significantly on annealing at temperatures above about 573 K.

4. Discussion

4.1. The effect of structural relaxation on T_c

As is evident from the results shown in Figs. 1 to 6, the feature of the change in T_c of amorphous $Nb_{70}Zr_{15}Si_{15}$ and $Zr_{85}Si_{15}$ alloys by thermal

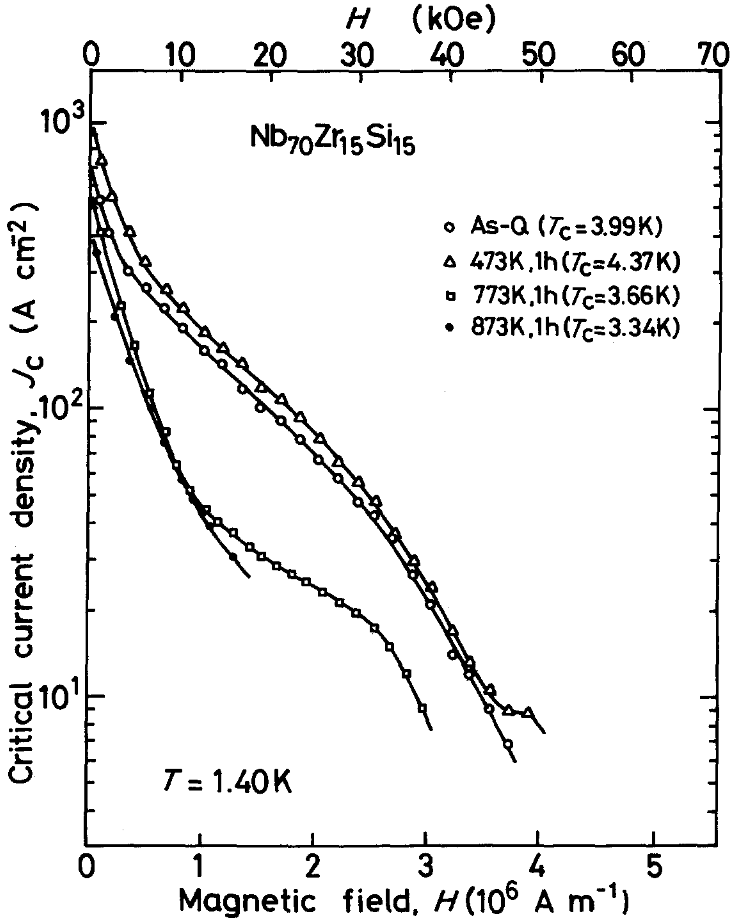

Figure 11 Critical current density, J_c, of an amorphous $Nb_{70}Zr_{15}Si_{15}$ alloy in as-quenched and annealed state as a function of magnetic field.

relaxation is summarized into the following two points. One is the change that T_c rises at temperatures below 473 K for the Nb–Zr–Si alloy and below 373 K for the Zr–Si alloy, and the other is the change that T_c lower monotonically in the ranges from 473 or 373 K to each crystallization temperature. The temperature ranges where the rise of T_c is observed are much lower than the crystallization temperature (1030 K for $Nb_{70}Zr_{15}Si_{15}$ [7] and 759 K for $Zr_{85}Si_{15}$ [7]) and hence it may be unreasonable to assume that the significant structural relaxation due to cooperative atomic regroupings occurs in the temperature range below 473 K. Instead of such an assumption, one may consider that voids, vacancies and/or the density fluctuations frozen by melt-quenching anneal out by annihilation and a short range change in the topological and/or chemical structure occurs even in such low-temperature ranges. On the other hand, the significant degradation of T_c at temperatures above 573 K is considered to be due to the structural relaxation accompanied by atomic rearrangements.

The ratio of the degradation of T_c, $\Delta T_c(t_a)/\Delta T_c(\infty)$, shown in Figs. 7 and 8 is considered to be proportional to the fraction of structural relaxation of an amorphous phase upon annealing. Consequently, it is possible to estimate an activation energy for relaxation which causes the degradation of T_c, if one assumes that the relaxation occurs by a single mechanism. Based on the relaxation curves of T_c shown in Figs. 7 and 8, the logarithm of $\tau_{1/2}$ in hours, which is the annealing time required to reach the midpoint on the T_c relaxation curve at a given annealing temperature, is plotted in Fig. 13 as a function of the inverse of the annealing temperature ($1/T_a$). There exists a good linear relation between $\ln[\tau_{1/2}(h)]$ and $1/T_a$ for a series of $Nb_{70}Zr_{15}Sr_{15}$ samples and hence the relation between $\tau_{1/2}$ and T_a is given by the following Arrhenius equation:

$$\tau_{1/2} = \tau_0 \exp(E/k_B T_a) \quad (1)$$

where E is the activation energy and k_B is the Boltzmann's constant. The activation energy determined from the slope in Fig. 13 was found to be

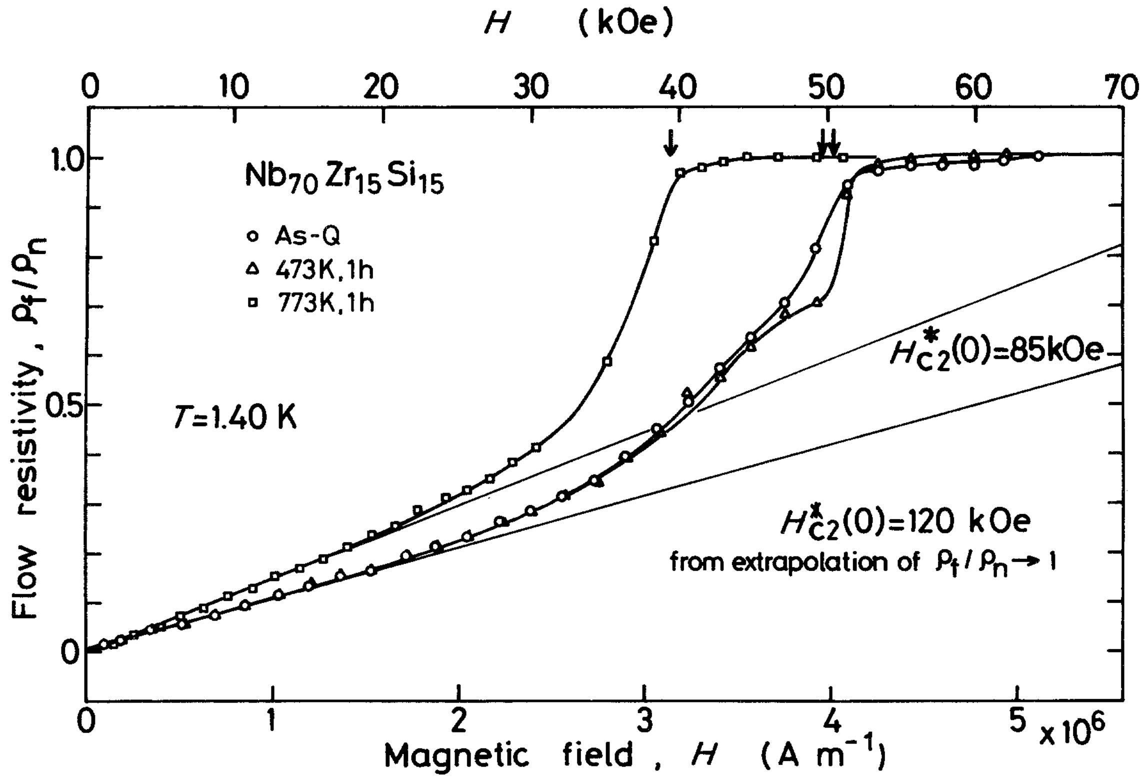

Figure 12 Normalized flux flow resistivity, ρ_f/ρ_n, of an amorphous $Nb_{70}Zr_{15}Si_{15}$ alloy in as-quenched and annealed state as a function of magnetic field.

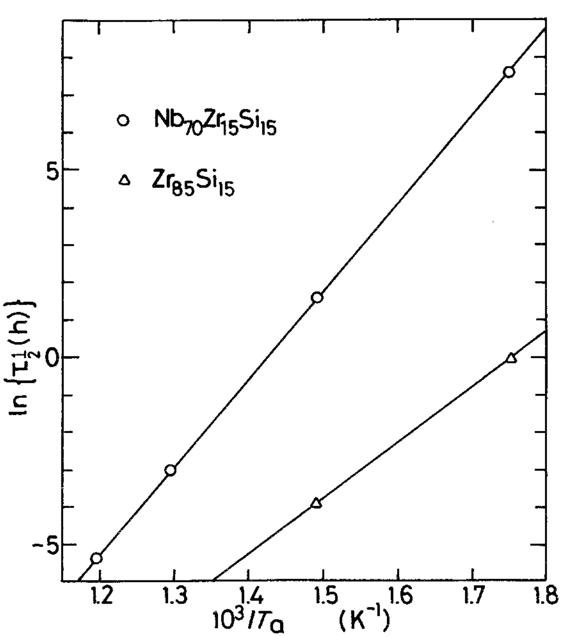

Figure 13 Arrhenius plot for determining the activation energy for the relaxation process for amorphous $Nb_{70}Zr_{15}Si_{15}$ and $Zr_{85}Si_{15}$ alloys.

2.03 eV for $Nb_{70}Zr_{15}Si_{15}$ and 1.28 eV for $Zr_{85}Si_{15}$, indicating that the lowering of T_c by structure relaxation is more difficult for the niobium-based alloy than for the zirconium-based alloy.

Using the activation energy one can estimate the frequency (ν) of the jump over this barrier by the following equation:

$$\nu = \ln 2 \frac{1}{\tau_0} \tag{2}$$

The ν value is estimated to be $2.4 \times 10^{14}\,\mathrm{sec}^{-1}$ for $Nb_{70}Zr_{15}Si_{15}$ and $1.2 \times 10^{11}\,\mathrm{sec}^{-1}$ for $Zr_{85}Si_{15}$. These ν values are nearly the same order as the Debye frequency (10^{13} to $10^{14}\,\mathrm{sec}^{-1}$). From this result it may be inferred that the structural relaxations which cause the degradation of T_c occur more or less independently of each other in a non-co-operative manner.

Next we shall estimate the dominating parameters for the superconductivity of the as-quenched and annealed alloys with an aim to investigate the microscopic origin of the change in the superconducting properties upon thermal relaxation.

According to McMillan's superconducting theory [12] which is applicable to an intermediate strong-coupling superconductor, T_c depends on the Debye temperature, Θ_D, and the electron–phonon coupling constant, λ; the larger the Θ_D and λ the higher is the T_c. The change in Θ_D by thermal relaxation is not directly measured in the present study. However, the previous data on the change in the Young's modulus sound velocity (V_E) by structural relaxation may allow one to predict the change in the Θ_D values upon annealing from the following equation based on the Debye approximation [13]:

$$V_E = \Theta_D \left(\frac{6\pi^2 N}{\Omega}\right)^{-1/3} = \frac{k_B \omega_D}{h}\left(\frac{6\pi^2 N}{\Omega}\right)^{-1/3}. \quad (3)$$

Here ω_D is the Debye phonon frequency and N/Ω the number of atoms per unit volume. There is established information that the V_E value increases by about 7% by structural relaxation [14]. Equation 3 clearly indicates that the increase in the Young's modulus sound velocity corresponds to the increase in the Debye phonon frequency and the Debye temperature. Considering the result that T_c lowers by the structure relaxation in spite of the increase in Θ_D, it is concluded that the degradation of T_c originates from the decrease in λ.

One can estimate the electronic dressed density of states at the Fermi level, $N^*(E_f) = N(E_f)(1 + \lambda)$, from the measured values of the H_{c2} gradient near T_c, $-(dH_{c2}/dT)_{T_c}$, and normal electrical resistivity, ρ_n, by using the following formula based on the Ginzburg–Landau–Abrikosov–Gorkov (GLAG) theory [15]:

$$N(E_f)(1+\lambda) = -\frac{\pi}{8k_B e \rho_n}\left(\frac{dH_{c2}}{dT}\right)_{T_c}. \quad (4)$$

The formula is applicable in the dirty limit where the electron mean free path is much less than the BCS superconducting coherence length $l \ll \xi_0$. It has been demonstrated that this criterion is well satisfied for the present amorphous superconductors [5, 6]. The values of $N(E_f)(1 + \lambda)$ thus obtained are plotted against annealing temperature in Fig. 14. The $N(E_f)(1 + \lambda)$ increases once on annealing at 473 K where T_c rises and then decreases significantly from 2.06×10^{47} to 1.82×10^{47} states m^{-3} J^{-1} $spin^{-1}$ in the temperature range of about 573 to 873 K where T_c lowers significantly. From this the change of T_c on annealing is interpreted

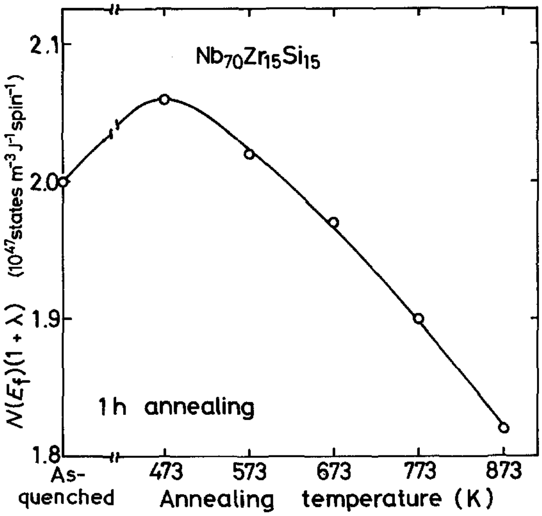

Figure 14 Change in the electronic dressed density of states at the Fermi level, $N(E_f)(1 + \lambda)$, of an amorphous $Nb_{70}Zr_{15}Si_{15}$ alloy with annealing temperature.

as due to the variation of λ or $N(E_f)$, being consistent with the conclusion derived from Equation 3.

The Eliashberg equation, which gives the accurate numerical solution of T_c, describes the relation between the λ and the phonon frequency ω as follows [12]:

$$\lambda = 2\int_0^\infty \alpha^2(\omega)F(\omega)\, d\omega/\omega \quad (5)$$

Here $F(\omega)$ is the phonon spectrum and $\alpha(\omega)$ the electron–phonon matrix element. Although there is no information on the change in the quantity $\alpha^2(\omega)F(\omega)$ for an amorphous phase by thermal relaxation, one can infer the change in λ on annealing by using McMillan's factorization of λ [12],

$$\lambda = \frac{N(E_f)\langle I^2\rangle}{M\langle\omega^2\rangle} \quad (6)$$

where $\langle I^2\rangle$ is the average over the Fermi surface of the square of the electronic matrix element, M the average ionic mass and $\langle\omega^2\rangle$ an average of the square of the phonon frequency. As is evident from Equation 6, the increase in ω_D and the decrease in $N^*(E_f)$ by structure relaxation result in a decrease in λ, even though the change in $\langle I^2\rangle$ by structure relaxation remains unknown for the present amorphous superconductor. From the above-described discussions, it is inferred that the degradation of T_c by structural relaxation originates from the decreases in λ and/or $N(E_f)$ and the

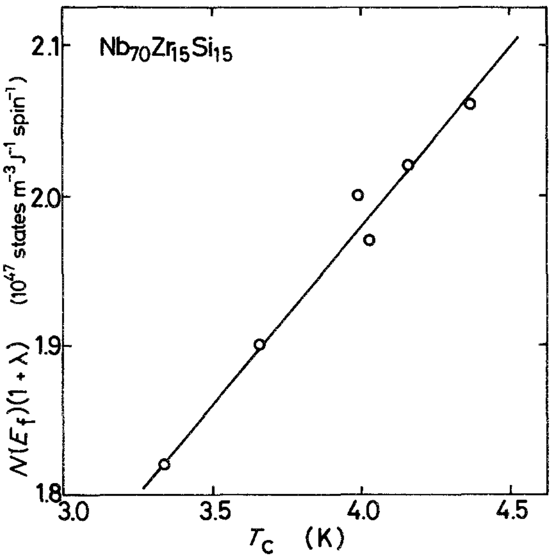

Figure 15 Correlation between $N(E_f)(1 + \lambda)$ and T_c for an amorphous $Nb_{70}Zr_{15}Si_{15}$ alloy in as-quenched and annealed state.

increase in $\langle\omega^2\rangle$. Further, Fig. 14 shows that $N(E_f)(1 + \lambda)$ also increases in the temperature range below about 573 K where T_c rises. This indicates that the rise of T_c corresponds strongly to the increases in $N(E_f)$ and λ. Although the reason why the change in $N(E_f)(1 + \lambda)$ with annealing separates into the two stages remains unknown, this result suggests that the electronic and phonon states in the amorphous phase change significantly in the vicinity of about 573 K. Fig. 15 shows the correlation between T_c and $N(E_f)(1 + \lambda)$ for a series of $Nb_{70}Zr_{15}Si_{15}$ samples in the as-quenched and annealed state. One can notice a strong correlation that the larger the $N(E_f)(1 + \lambda)$ value the higher is the T_c.

4.2. Effect of structural relaxation on $J_c(H)$

As shown in Fig. 12, the $J_c(H)$ of the $Nb_{70}Zr_{15}Si_{15}$ amorphous alloy increases slightly on annealing for 1 h at 473 K and decreases significantly with further rising annealing temperature. Since such changes in $J_c(H)$ for the annealed samples are considered to reflect the change in T_c, the rearrangement in which the influence of T_c is not involved was tried. Based on the data shown in Fig. 12, the normalized fluxoid pinning force, $F_p/F_{p\,max}$, as a function of magnetic field, B/H_{c2}, was plotted in Fig. 16, where F_p is calculated by $B \times J_c$ and $F_{p\,max}$ represents the largest F_p for the as-quenched

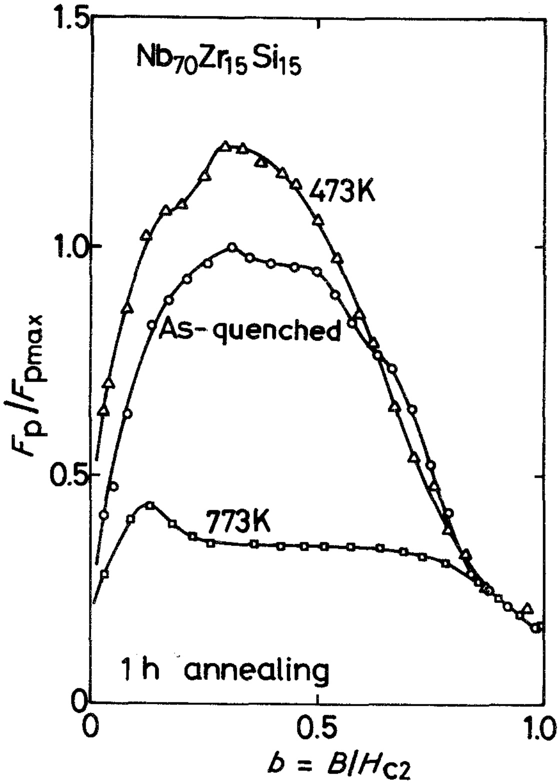

Figure 16 Normalized fluxoid pinning force, $F_p/F_{p\,max}$, of an amorphous $Nb_{70}Zr_{15}Si_{15}$ alloy in as-quenched and annealed state as a function of magnetic field, $b = B/H_{c2}$. $F_{p\,max}$ represents the largest F_p for the as-quenched sample.

sample. This figure may be summarized as follows. 1. The fluxoid pinning force increases once by about 20% on annealing at 473 K and decreases to about $0.6F_{p\,max}$ on annealing at 773 K. 2. The value of B/H_{c2} where F_p shows a maximum value decreases largely from about 0.30 for the as-quenched and annealed (473 K x 1 h) samples to 0.13 for the sample annealed at 773 K, implying that the annealing at temperatures above about 573 K causes a significant decrease in fluxoid pinning force in applied magnetic field. These results indicate clearly that the relaxation from the quenched-in structure into a more stable and homogeneous state on annealing at temperatures above about 573 K causes an increase in the homogeneity in the amorphous structure on the scale of coherence length ($\simeq$ 7.5 nm), resulting in a significant decrease in the fluxoid pinning force. Although the reason why the fluxoid pinning force increases slightly on annealing at a temperature as low as 473 K is not clear, it may be considered as follows: an extremely large number of quenched-in microdefects such as vacancies, voids and the density fluctuations rearrange and coalesce, even on annealing at a low temperature around 473 K. As a result, the size of such defects is almost equal to the coherence length (7 to 8 nm) and they act as effective fluxoid pinning centres, resulting in slight increases in $J_c(H)$ and fluxoid pinning force. The detailed investigation on the structural change in amorphous phase on annealing at low temperatures below about 473 K will shed some light upon the further understanding of the mechanism on the enhancement of the fluxoid pinning force.

5. Summary

The effect of thermal relaxation on the superconducting properties of an amorphous phase was examined by using $Nb_{70}Zr_{15}Si_{15}$ and $Zr_{85}Si_{15}$ amorphous samples. The results obtained are summarized as follows.

1. On isochronal or isothermal annealing, T_c rose from 3.99 to 4.42 K at temperature below about 473 K for the Nb–Zr–Si alloy and from 2.71 to 2.75 K at temperatures below 373 K for the Zr–Si alloy and with further rising annealing temperature lowered monotonically to a final relaxed value ($\simeq 3.15$ K for $Nb_{70}Zr_{15}Si_{15}$ and $\simeq 2.49$ K for $Zr_{85}Si_{15}$), which was independent of the previous thermal cycling. This indicates that the thermal relaxation of an amorphous phase occurs through at least two stages. Further, it was interpreted that the rise of T_c in a low-temperature range is due to the annihilation of quenched-in defects such as vacancies, voids and the density fluctuations, while the degradation of T_c in a higher temperature range occurs by structural relaxation accompanied by atomic regroupings.

2. The degradation of T_c occurred exponentially with annealing temperature, and an activation energy for the relaxation process was about 2.03 eV for $Nb_{70}Zr_{15}Si_{15}$ and about 1.28 eV for $Zr_{85}Si_{15}$. The frequency of jump over the barrier was about 2.4×10^{14} sec^{-1} for the niobium-based alloy and about 1.2×10^{11} sec^{-1} for the zirconium-based alloy. The high frequencies indicate that the relaxation occurs more or less independently of each other in a non-co-operative manner.

3. The dressed density of electronic states at the Fermi level, $N(E_f)(1+\lambda)$, which was calculated from the measured values of ρ_n and $-(dH_{c2}/dT)_{T_c}$ by using the GLAG theories, exhibited a similar annealing temperature dependence to that of T_c. From this it was interpreted that the change in T_c on thermal relaxation originates from the changes in λ and/or $N(E_f)$.

4. The $J_c(H)$ of $Nb_{70}Zr_{15}Si_{15}$ alloy decreases and the $\rho_f(H)$ increases on annealing at temperatures above about 573 K. From these changes it was concluded that the atomic regroupings from an unrelaxed inhomogeneous state in the quenched-in structure to a relaxed homogeneous state resulted in a depression of fluxoid pinning force as well as a lowering of T_c.

References

1. H. S. CHEN, *Rep. Prog. Phys.* **43** (1980) 353.
2. A. J. DREHMAN and W. L. JOHNSON, *Phys. Status Solidi* **52** (a) (1979) 499.
3. A. RAVEX, J. C. LASJAUNIAS and O. BETHOUX, *Physica* **107B** (1981) 397.
4. C. C. KOCH, D. M. KROEGER, J. S. LIN, J. O. SCARBROUGH, W. L. JOHNSON and A. C. ANDERSON, *Phys. Rev.* **27** (1983) 1586.
5. A. INOUE, Y. TAKAHASHI, N. TOYOTA, T. FUKASE and T. MASUMOTO, Proceedings of the 4th International Conference on Rapidly Quenched Metals, Sendai, August 1981, Vol. II, edited by T. Masumoto and K. Suzuki (The Japan Institute of Metals, 1982) p. 1221.
6. *Idem, J. Mater. Sci.* **18** (1983) 114.
7. A. INOUE, Y. TAKAHASHI, C. SURYANARAYANA and T. MASUMOTO, *ibid.* **17** (1982) 3253.
8. A. INOUE, S. SAKAI, H. M. KIMURA and T. MASUMOTO, *Trans. Jpn. Inst. Met.* **20** (1979) 255.
9. A. INOUE, Y. TAKAHASHI and T. MASUMOTO, *Sci. Rep. Res. Inst. Tohoku Univ.* **A-29** (1981) 296.
10. A. INOUE, Y. TAKAHASHI, A. HOSHI and T. MASUMOTO, Proceedings of the 4th International Conference on Rapidly Quenched Metals, Vol. II, edited by T. Masumoto and K. Suzuki (Japan Institute of Metals, 1982) p. 1249.
11. Y. B. KIM, C. F. HEMPSTEAD and A. R. STRNAD, *Phys. Rev.* **139** (1965) A1163.
12. W. L. McMILLAN, *ibid.* **167** (1968) 331.
13. T. OTUKA, "Ferroelectrics and Superconductors" (The Japan Institute of Metals, Sendai, 1973) p. 131.
14. H. S. CHEN, *J. Appl. Phys.* **49** (1978) 3289.
15. For example, T. P. ORLANDO, E. J. McNIFF Jr, S. FORNER and M. R. BEASLEY, *Phys. Rev. B* **19** (1979) 4545.
16. N. TOYOTA, T. FUKASE, A. INOUE, Y. TAKAHASHI and T. MASUMOTO, *Physica* **107B** (1981) 465.

Received 24 October and accepted 19 December 1983